Langmuir

Article

pubs.acs.org/Langmuir

Formation of Rectangular Packing and One-Dimensional Lines of C_{60} on 11-Phenoxyundecanethiol Self-Assembled Monolayers on Au(111)

Miki Nakayama, Natalie A. Kautz, Tuo Wang, and S. J. Sibener*

The James Franck Institute and Department of Chemistry, The University of Chicago, 929 E. 57th Street, Chicago, Illinois 60637, United States

ABSTRACT: The behavior of C_{60} molecules deposited onto 11-phenoxyundecanethiol (phenoxy) self-assembled monolayers (SAMs) is studied using ultrahigh vacuum scanning tunneling microscopy (UHV-STM) and spectroscopy. We observe that after thermally annealing between 350 and 400 K in vacuum a combination of hexagonally close-packed islands, rectangularly packed islands, and isolated single lines of C_{60} is observed when the C_{60} is initially deposited on an unannealed phenoxy SAM. However, only rectangularly packed islands are found when they are deposited on a preannealed phenoxy SAM. We determine the rectangular packing to have a $(2\sqrt{3} \times 4)$ rectangular unit cell with respect to the underlying Au(111) substrate. This type of C_{60} structure has not been observed previously for multicomponent self-assemblies on a surface. We discuss the possible causes for the formation of this structure as well as the differences between starting on an unannealed SAM and an annealed one. This study demonstrates the capability of functionalized alkanethiol SAMs to control the growth and structure of C_{60} islands during annealing depending on the structural changes of the SAM itself; by preannealing the SAM, the motion of the C_{60} can be confined and unique structures resulting from interactions between the SAM molecules and C_{60} can be produced.

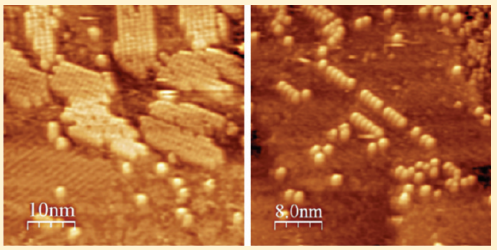

INTRODUCTION

Ever since their official discovery in 1985,[1] C_{60} fullerenes have attracted much attention due to their unique shape, size, and chemical and physical properties.[2−5] The spherical delocalization of their π-electrons results in interesting optical properties and the ability to conduct electricity.[6,7] Also, their alkene-like chemical reactivity allows functionalization of the molecule,[8] making their properties tunable. These characteristics make C_{60} an excellent candidate for use in applications such as solar cells and molecular electronics.[9−12]

Technological applications of C_{60} typically involve depositing them onto a surface, and therefore numerous studies have been done of C_{60} on surfaces ranging from metals[13−15] to semiconductors[16−18] to polymers.[19,20] Adsorption on Au(111) has especially been well-investigated because C_{60} forms highly ordered films on it without chemisorption. Initially, $(2\sqrt{3} \times 2\sqrt{3})$R30° and 38 × 38 in-phase structures were reported,[21] and since then, a (7×7)R14° structure has additionally been found.[22,23] More recently, a (3×3)R34° structure has also been proposed.[24] In all of these structures, the C_{60} molecules are hexagonally close-packed, but the adsorption sites of the molecules are different.

Along with the physical structure, it is also important to understand how the C_{60}'s electronic structure is affected by the neighboring molecules and the substrate. Scanning tunneling spectroscopy (STS) is especially well-suited for these studies because it can probe the electronic structure of a single C_{60} molecule in different environments on a sample. By taking dI/dV curves, the HOMO and LUMO positions can be determined. It has been shown previously that the HOMO−LUMO gap is about 2.8 eV for a single C_{60} molecule on Au(111) located away from any steps, but the gap reduces to 2.4 eV due to a shift of the LUMO peak when the C_{60} is surrounded by six other molecules in a close-packed island due to screening effects.[25] Even within a monolayer, the LUMO peak shifts 0.1 eV toward higher energies when the C_{60} is located at the lower part of a step edge.[26] The HOMO−LUMO gap is also greatly affected by the substrate. For example, it is about 2.1 eV on Ag(100), which is a significant reduction from Au(111).[27] This is because silver has a lower work function relative to gold which results in more charge transfer to the C_{60}, thereby increasing the screening effect.[27]

For technological applications of C_{60}, it is desirable to be able to control the extent of coupling between the C_{60} and the substrate and to be able to arrange the molecules into desired structures or patterns. In order to achieve these goals, many studies have been conducted on multicomponent assemblies, usually involving depositing C_{60} on top of a molecular monolayer on a metal substrate which serves as a template and/or a dielectric spacer. C_{60}-porphyrin assemblies have been particularly popular because they form host−guest complexes, mainly through dispersion and donor−acceptor interactions.[28] Various other molecules involving electron-rich aromatic rings have been used as well. For example, when C_{60} is deposited

Received: December 17, 2011
Revised: February 8, 2012
Published: March 2, 2012

   dx.doi.org/10.1021/la204986n | *Langmuir* 2012, 28, 4694−4701

onto a monolayer of *p*-sexithiophene on Ag(111), the donor−acceptor interaction between them constrains the C_{60} to adsorb with a hexagon facing down.[29] When C_{60} is codeposited with 1,3,5,7-tetraphenyladamantane on Au(111), triangular tetramers with a C_{60} molecule in the center are formed due to attractive electrostatic interactions.[30] The C_{60} molecules are lifted slightly from the surface in these tetramers, and this is reflected in their STS measurements, where the HOMO−LUMO gap is about 2.6 eV and the LUMO peak becomes significantly sharper compared to that of C_{60} sitting directly on a metal.[30] They also observe a region of negative differential resistance where the current decreases with increasing sample bias, which is another indication that the coupling of the C_{60} to the substrate is very weak.[30] In this work, we study the capability of phenoxy-terminated SAMs to act as a template for C_{60} growth.

C_{60} has been deposited onto alkanethiol SAMs on Au(111) as well and studied with STM to see whether the SAMs can be used to decouple the C_{60} from the gold or act as a template. When Hou et al. vapor-deposited C_{60} onto an alkanethiol SAM of unspecified chain length at room temperature, they obtained hexagonally close-packed arrays of C_{60}.[31] They assumed that the C_{60} were sitting on top of the SAM because the molecules appeared smooth, suggesting that they were freely rotating as opposed to on metals or semiconductors where the rotation can be frozen even at room temperature.[31] They did not report the apparent height of the C_{60}. In contrast, Li et al. have vapor-deposited C_{60} onto an octanethiol SAM at room temperature and observed that the C_{60} do not form close-packed islands, but instead all scatter at defect sites and lower coverage areas of the SAM.[32] On the basis of the C_{60}'s apparent height of 4 Å above the SAM, they concluded that the C_{60} are sitting directly on the gold substrate.[32] It is not clear whether the difference of the two studies is due to possibly different chain lengths of alkanethiols used or to different amounts of C_{60} deposited onto the surface. STS measurements were not made for either of these studies. Another study has shown that when the C_{60} are deposited onto a hexanethiol SAM at 78 K, hexagonally close-packed islands form on top of the SAM.[33] The C_{60}'s apparent height was not reported, but *I*−*V* curves were taken which show that the HOMO−LUMO gap ends at a little below 1.5 V on the LUMO side.[33] This shows that the LUMO is shifted higher than for C_{60} islands on bare Au(111), which indicates less screening from the immediate environment, consistent with the picture that the C_{60} are sitting on top of the SAM, away from the screening effects of the gold surface.[25] C_{60} has also been previously deposited on top of mixed intermediate stripe phases of decanethiol SAMs at 78 K, and it was found that most of the C_{60} formed bimolecular chains along the stripes that were spaced 1.9 nm apart.[34] It was suggested that the C_{60} molecules were sitting on top of the S-terminus sites and held in place by bent molecules forming furrows.[34] Neither the apparent height nor the STS measurements of the C_{60} were reported for this structure.

In addition to decoupling the C_{60} from the metal substrate, by utilizing SAMs terminated by a functional group, the properties of the C_{60} can potentially be controlled as well as their orientation and structure on the SAM. Several groups have studied C_{60} on functionalized SAMs, typically involving an amine group for chemisorption. C_{60} has been shown to react with the amine group on a $HS(CH_2)_2NH_2$-modified gold substrate to form a monolayer on top of the SAM.[35] Later, Sahoo and Patnaik attached C_{60} onto a longer 8-amino-1-octanethiol SAM on gold and were able to confirm that the amino group binds at the 6:6 bond of the C_{60} molecule using Fourier transform infrared-attenuated total reflection spectroscopy and X-ray photoelectron spectroscopy.[36] It has also been shown with atomic force microscopy that C_{60} attach firmly to azide-terminated SAMs on silicon to form a regular, close-packed multidomain structure on the SAM.[37]

In this work, we conduct STM and STS studies of C_{60} deposited on an as-prepared 11-phenoxyundecanethiol (phenoxy) SAM in its dense phase and on a thermally annealed phenoxy SAM in its $(5 \times \sqrt{3})$ stripe phase to study their capability of acting as a template for C_{60}. The behavior of C_{60} on functionalized alkanethiol-based SAMs is still not very well understood, especially on those involving aromatic groups. Aromatics groups are especially interesting as noted above because significant interactions can occur without the formation of chemical bonds. Here, we observe that highly unique rectangularly packed islands are formed when the C_{60} are annealed in vacuum on the stripe phase phenoxy SAM, and one-dimensional single lines of C_{60} are formed when they are annealed on an as-prepared phenoxy SAM, along with some of the rectangularly packed islands and the more familiar hexagonally close-packed islands. We believe that the difference on the two surfaces is due to the more drastic changes that the SAM goes through when it is annealed for the first time, and we propose that the rectangular packing is a result of $\pi-\pi$ interactions between the C_{60} and the phenoxy group and the limited motion they encounter at domain boundaries and defect sites. The ability to control the surface structure of C_{60} using aromatic SAMs will contribute to making desired hierarchical structures for real-life applications.

EXPERIMENTAL SECTION

Sample Preparation. 1 mM solutions of 11-phenoxyundecanethiol (phenoxy) in ethanol were purchased from Asemblon Inc. and used without any further treatment. Au(111)/mica substrates were purchased from Agilent Technologies. These are gold films of at least 1500 Å epitaxially grown on cleaved mica. The substrates were cleaned by hydrogen-flame-annealing prior to use. C_{60} (sublimed, 99.9%), benzene (anhydrous, 99.8%), and ethanol (200 proof, anhydrous) were purchased from Sigma-Aldrich and used as-is.

The phenoxy SAMs were formed by soaking the Au(111) substrates in the 1 mM solution for over 48 h at room temperature. The solutions were kept in the dark. After immersion, the samples were rinsed well with ethanol and dried under a stream of nitrogen gas to get rid of any physisorbed material. The quality of the SAMs was checked with STM before depositing C_{60} on them.

C_{60} stock solutions were made by dissolving ∼0.5 mg of C_{60} in 10 mL of benzene. A stock solution was used for no more than 2 weeks. The stock was diluted 20−50-fold with benzene right before use. A ∼5 μL drop of the diluted solution was drop-cast onto the substrate using a micropipet and then left out in air to dry. The drying process typically only took about a minute.

Annealing of the samples was done *in situ* in our STM chamber (described below) using radiative heating from a tungsten filament mounted directly underneath the sample. The temperature was monitored by a K-type thermocouple mounted on the sample surface for accurate measurement. The samples were usually left to cool back to room temperature overnight in UHV to minimize thermal drift during STM measurements.

STM/STS Measurements. STM measurements were made in a UHV 300 system (RHK Technology, Inc.) which houses a Besocke beetle, or "walker," style STM. The base pressure of the chamber was less than 5×10^{-10} Torr. The STM tips were made either by mechanically cutting or chemically etching a PtIr wire (Pt80/Ir20, Goodfellow). Typical imaging parameters were 10 pA tunneling

dx.doi.org/10.1021/la204986n | *Langmuir* 2012, 28, 4694−4701

current and around 0.7 V sample bias unless otherwise noted. All measurements were made at room temperature. STS measurements were made at preselected points within an STM image. As the imaging reaches the preselected points, the feedback loop is temporarily suspended while $I-V$ curves are obtained. In this way, it is possible to know exactly where the STS measurements were taken. dI/dV curves were obtained either numerically by differentiating the $I-V$ curves using the image acquisition software or directly by using a lock-in amplifier with rms modulation of 20 mV at 1 kHz. Data from whichever method that gave the most consistent and highest sensitivity results for a given measurement are presented here.

RESULTS

We have deposited C_{60} onto both an unannealed and an annealed phenoxy SAM. The structure of the phenoxy SAMs has been described in detail elsewhere,[38] and only the main aspects will be summarized here. A freshly prepared phenoxy SAM has an alkyl chain layer which is relatively densely packed and well-ordered with a chain tilt angle of about 30° from the surface normal, similar to that of a normal unsubstituted alkanethiol SAM. The phenoxy terminal groups are forced to be largely perpendicular to the surface, but they are not locally crystalline, making the phenoxy SAM look disordered under the STM. When the phenoxy SAM is annealed above 350 K, a $(5 \times \sqrt{3})$ striped phase is formed that is slightly less dense. The alkyl chains are tilted 50° from the surface normal, and the stripes consist of pairs of molecules with favorably interacting phenyl rings. STM images of a phenoxy SAM before and after annealing are shown in Figure 1.

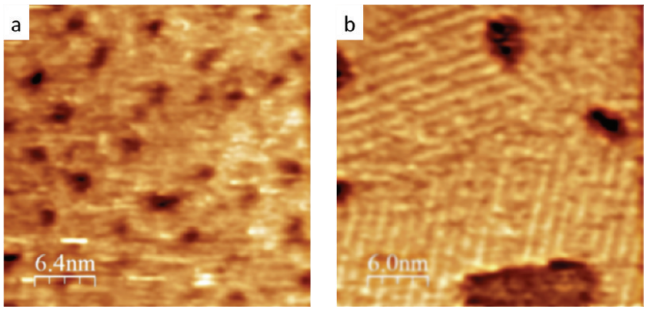

Figure 1. (a) A 32.6 × 32.6 nm^2 STM image of an as-prepared phenoxy SAM, acquired at 1.3 V and 10 pA. (b) A 32.0 × 32.0 nm^2 STM image of an annealed phenoxy SAM, acquired at 1.4 V and 10 pA. Before annealing, the surface appears disordered and small etch pits are scattered about (a), but after annealing, domains of $(5 \times \sqrt{3})$ striped phase appear, and the etch pits have coalesced into larger ones (b).

First, we deposited C_{60} onto an annealed phenoxy SAM with the $(5 \times \sqrt{3})$ striped phase to examine its capability to act as a template. An STM image of as-deposited C_{60} on the phenoxy stripes is shown in Figure 2a. The C_{60} have an apparent height of about about 4 Å on average above the stripes, and they seem to be scattered about without any particular preference to align along the stripes. The images often contained streaks, indicating that the C_{60} are mobile. When the sample was annealed between 350 and 400 K in UHV, ~4 Å high islands of C_{60} packed in a rectangular pattern appeared as shown in Figure 2b. The C_{60} in these islands are close-packed in one direction with a spacing of 10 Å, but slightly less so in the other with a measured spacing of 11.5 Å on average. The close-packed direction either follows the phenoxy stripes or is rotated 120° from them, which means the C_{60} are close-packed in the ⟨121⟩ direction of the underlying Au(111) surface just like the stripes.[38] 11.5 Å matches the distance between four adjacent gold atoms, so the C_{60} are packed in a $(2\sqrt{3} \times 4)$ rectangular pattern with respect to the gold substrate. The islands were usually longer in the close-packed direction, and dark spots were frequently found within. These dark spots could either be missing molecules or C_{60} molecules that appear dark. The appearance of dim C_{60} in islands or monolayers has been reported previously,[21,23] and it has recently been proposed that it is due to the formation of nanopits from the restructuring of the gold atoms underneath to facilitate charge transfer to the C_{60}.[24] Sometimes there were domains within islands where they were shifted by half a unit cell from each other as shown in Figure 2b. We also observed that there were islands that were stable over time and ones that started to dissociate immediately after scanning over them. The islands with the longer close-packed edge exposed to a large area of the phenoxy stripes appeared to be especially vulnerable to dissociation.

For comparison, we also deposited C_{60} onto an unannealed phenoxy SAM. In the as-deposited state, the C_{60} were scattered about much like on the striped phenoxy SAM as in Figure 2a, with an apparent height of around 4−5 Å above the SAM. The STM images were often streaky, indicating that the C_{60} are mobile on the unannealed SAM as well. However, when the sample was annealed in UHV between 350 and 400 K, the resulting surface looked different from when the C_{60} were initially deposited on to the annealed striped phenoxy SAM. STM images of the annealed surface are shown in Figure 3. The $(2\sqrt{3} \times 4)$ rectangular islands existed but only in very small sizes usually only two to three rows wide, and bigger ones seemed to appear only in Au-monatomic-deep pits. Most of the C_{60} islands were hexagonally close-packed, and many of them resembled a triangle with the edges running along the ⟨121⟩ direction of the underlying gold substrate based on the direction of the phenoxy stripes, as shown in Figure 3b. This corresponds to a $(2\sqrt{3} \times 2\sqrt{3})$R30° structure which has been found to be the most stable structure of C_{60} islands on bare Au(111).[32,39] The most striking feature of the surface after annealing was single lines of C_{60} running along the phenoxy stripes, some of them extending up to greater than 20 nm in length. The C_{60} were close-packed along the lines and appeared to hardly disturb the surrounding phenoxy stripes as shown in Figure 3c,d. All of the C_{60} features on the annealed surface had an apparent height of about 4−5 Å above the phenoxy SAM, and they were relatively stable against imaging. It can also be seen that except for the lines, C_{60} islands and clusters are mostly located in domain boundaries of the phenoxy SAM.

In order to gain insight into how the electronic states of the C_{60} are affected by the presence of the phenoxy SAM, we took STS measurements on the rectangular and hexagonal C_{60} structures observed. The resulting dI/dV curves are shown in Figure 4 along with spectra taken on a large hexagonally close-packed island on bare Au(111) for comparison. Even though the C_{60} single lines were usually stable against imaging, they were heavily affected by STS measurements, and we were not able to obtain consistent spectra over them. Our data for C_{60} on bare Au(111) show that the HOMO peak lies at −1.7 V and the LUMO peak at 1.0 V. These values correspond well to those previously reported for C60 in close-packed islands where the molecules were spray coated onto Au(111) on mica.[40] The LUMO peak position is slightly shifted from other reports of around 0.7 V for C_{60} islands where the molecules were vapor-dosed in UHV onto single crystal Au(111).[25,27] We potentially

dx.doi.org/10.1021/la204986n | Langmuir 2012, 28, 4694−4701

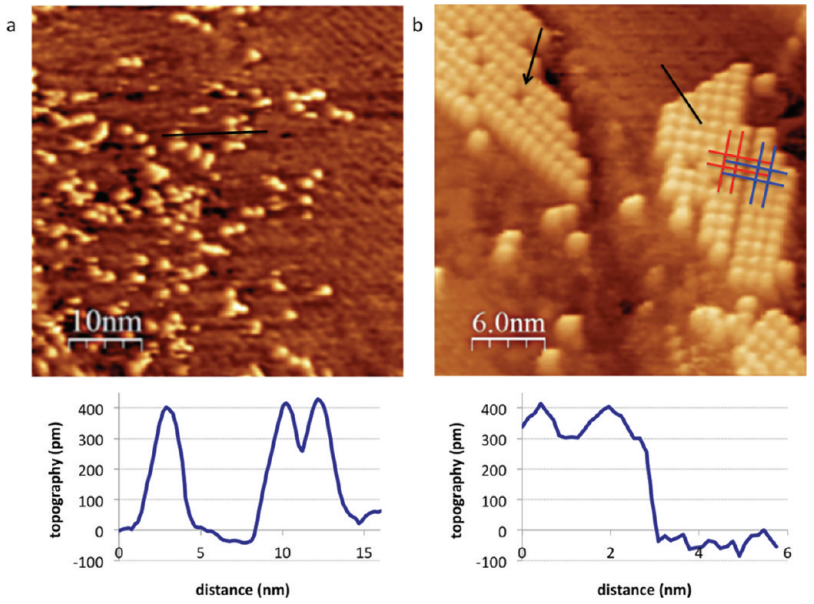

Figure 2. (a) A 50 × 50 nm^2 STM image of C_{60} deposited on an annealed phenoxy SAM in the as-deposited state, acquired at 0.9 V and 10 pA. The C_{60} molecules appear scattered, and there are streaks in the image indicating the C_{60} are mobile. A line scan along the line is shown on the bottom. (b) A 30 × 30 nm^2 STM image of the rectangularly packed C_{60} islands formed after annealing in vacuum, acquired at 0.7 V and 10 pA. The black arrow is pointing at an example of an apparent missing molecule in the island. The red and blue lines are drawn over the C_{60} molecules in each of the respective domains in the island and then extended over to the other domain to clarify that the domains are shifted by half a unit cell. A line scan along the black line is shown on the bottom.

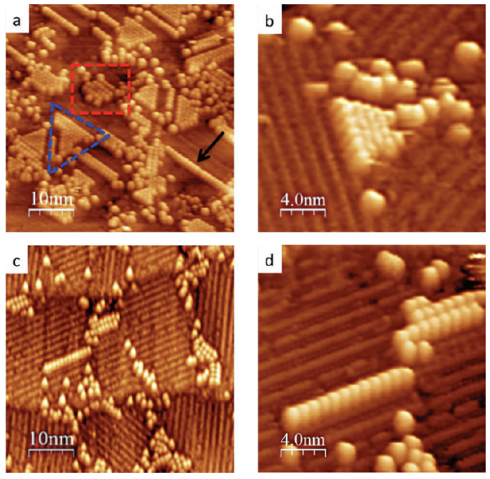

Figure 3. STM images of C_{60} deposited on an as-prepared phenoxy SAM and then annealed in vacuum: (a) 50 × 50 nm^2, acquired at 0.7 V and 13 pA. The arrow is pointing at an example of a one-dimensional single C_{60} line. The blue triangle is placed around a $(2\sqrt{3} \times 2\sqrt{3})R30°$ hexagonally close-packed island. The red rectangle is placed around a rectangularly packed island in a pit. (b) A 20 × 20 nm^2 image of a $(2\sqrt{3} \times 2\sqrt{3})R30°$ structure island where domains of the phenoxy stripes surrounding it are visible, acquired at 0.7 V and 10 pA. (c) Another 50 × 50 nm^2 area where domains of stripes are visible, and most of the C_{60} are at the domain boundaries. (d) A 20 × 20 nm^2 zoomed-in image of the C_{60} line in (c), acquired at 0.7 V and 10 pA.

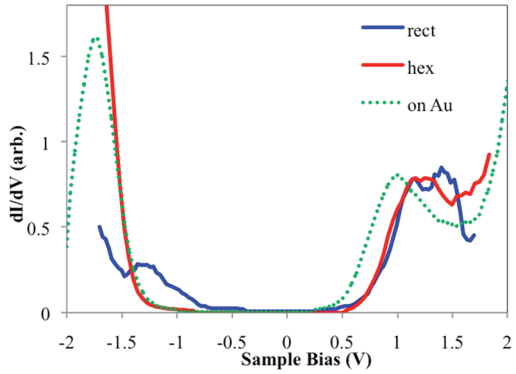

Figure 4. dI/dV curves of the C_{60} hexagonally close-packed islands and rectangularly packed islands, along with that of a hexagonally close-packed island on bare Au(111) for comparison. The data for the rectangularly packed island were obtained by numerical differentiation of the $I-V$ curve using the data acquisition software, and the other two curves were taken directly using a lock-in amplifier. The curves for rectangular packing, hexagonal packing, and hexagonal packing on bare Au(111) are averages of 8, 27, and 64 individual curves, respectively. It can be seen that the LUMO peak is shifted to higher energies for both structures on the phenoxy SAM.

attribute this difference to substrate effects. It has been noted before that the position of the surface state is slightly different between single crystal Au(111) and Au(111) on mica, most likely due to mechanical stress.[41] This may affect the C_{60}–Au(111) interaction, which in turn may affect the C_{60}'s LUMO position. Since all of our experiments are done on Au(111) on mica using solution deposition, the relative positions of the peaks should not be affected.

From the spectra in Figure 4, we can see that the LUMO position shifted higher for both hexagonally packed and rectangularly packed islands of C_{60} on the phenoxy SAM. The peak for the hexagonal islands shifted to about 1.2 V. The peak for the rectangular islands is centered around 1.3 V, and it appears to be split. Upward shifts of the LUMO have been observed previously in literature for C_{60} experiencing less screening effects at island or step edges, isolated molecules, or molecules lifted from the metal substrate.[25,26,40] Broadening or splitting of the HOMO and LUMO peaks are an indication of

dx.doi.org/10.1021/la204986n | *Langmuir* 2012, 28, 4694–4701

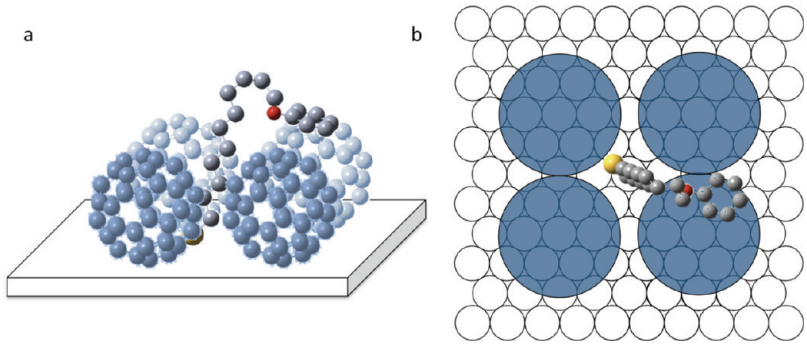

Figure 5. (a) Side view of a schematic of a possible structure of the $(2\sqrt{3} \times 4)$ rectangular islands. The phenoxy molecule's phenyl ring is interacting with a C_{60} molecule. The two C_{60} molecules in the back are greyed out for clarity of depth. (b) Top view of the same schematic. The transparent dark blue circles represent C_{60} molecules with their van der Waals radius, and the white circles are the Au surface atoms. The adsorption sites with respect to the gold lattice are for schematic purposes only.

increased interaction with the substrate or neighboring molecules, resulting in increased screening or distortion of the molecular cage due to Jahn–Teller effects which lifts the degeneracy of the MOs.[25,42] The HOMO peak location is unclear for the hexagonal islands on the phenoxy SAM, and it looks as though there is a shoulder at around 1.3 V for the rectangular islands, but HOMO peaks are generally heavily affected by the tip's unoccupied electronic structure,[25,43] and we cannot eliminate the possibility of SAM molecules on the tip affecting their appearance, especially for the case of rectangular islands where phenoxy molecules are interspersed within the structure as will be discussed below. Therefore, the HOMO peaks will not be discussed further to understand the behavior of C_{60} on the phenoxy SAM for this study.

DISCUSSION

The first question we need to address is whether the C_{60} molecules are sitting on top of the phenoxy SAM or are buried inside and sitting directly on the gold substrate. We deposited the C_{60} at room temperature, and the apparent height always stayed around 4 Å both before and after annealing, which matches what Li et al. observed for C_{60} sitting on gold inside an octanethiol SAM at room temperature.[32] We believe that this is a strong indication that the C_{60} molecules are buried in the SAM and sitting on the gold substrate. If the C_{60} were sitting on top of the SAM, we would expect the apparent height relative to the SAM to be much higher because C_{60} should be more conductive than the SAM; the limiting step of the tunneling process should be through the least conductive part which is the alkyl chain. The exception would be if there is significant charge transfer to the C_{60} from the phenoxy groups which would make it more difficult for electrons to tunnel through the C_{60}, making it appear dimer or lower. However, that is rather unlikely because although the ether moiety has an electron-donating resonance effect on the phenyl ring, it has an electron-withdrawing inductive effect.[44]

Another reason we believe the C_{60} molecules are sitting directly on the gold substrate is that the C_{60} form structures that are commensurate with Au(111) after annealing, and not with the phenoxy stripes, except for the single lines which are commensurate with both. In particular, all of the hexagonal patches that we have observed are in the $(2\sqrt{3} \times 2\sqrt{3})$R30° structure which is strong evidence for direct C_{60}–Au(111) interaction.[32] Also, in Figure 3, it can be seen that most of the C_{60} are located in between the domains of the phenoxy stripes, suggesting that they are not sitting on top of the stripes.

Our STS results also indicate that the C_{60} are sitting on the gold. The C_{60} LUMO peaks for both the hexagonally packed and rectangularly packed islands have shifted higher to about 1.2 or 1.3 V from around 1.0 V for close-packed islands on bare Au(111), indicating less screening from their environment. However, we would expect the shift to be greater if they were sitting on top of the SAM based on what was reported for C_{60} islands on a hexanethiol SAM, where it looks like the LUMO peak is between 1.5 and 2.0 V from the I–V curve.[33] The shift of the hexagonally packed islands on the SAM was somewhat unexpected since the local environment should be the same as on bare Au(111), but the islands were typically very small on the SAM, and even if we picked C_{60} molecules in the middle, most of their neighbors were on the edge of the island and may not have been able to provide the same screening effects. Also, if the C_{60} were lifted away from the gold, we would expect a sharper LUMO peak with smaller fwhm due to less interactions and less distortion of the molecule,[25,30] but this was not the case.

From the above observations, we can propose what happens to the C_{60} as they are deposited on the phenoxy SAM and annealed with it. First, on the annealed striped phenoxy SAM, the deposited C_{60} do not appear to interact strongly with the phenoxy groups and instead diffuse around and find defect sites to burrow down to the gold substrate, where the C_{60}–Au(111) adsorption energy is estimated to be around 40–60 kcal/mol.[21,45] When the C_{60} are deposited onto bare Au(111), they normally diffuse to step edges,[21] but in the phenoxy SAM, the phenoxy molecules hinder free diffusion.[32,46] The streaks in the STM images indicate however that the C_{60} molecules do have limited motion within the SAM, probably because there is more open space within the striped SAM, especially with defects, relative to a standing phase alkanethiol SAM.

When the C_{60} and phenoxy SAM are annealed above 350 K, $(2\sqrt{3} \times 4)$ rectangular islands of C_{60} are formed. As far as we know, this kind of C_{60} packing has not been observed previously for a hierarchical assembly on a surface. The formation of these rectangular islands indicates that there is a configuration where relatively significant interactions between the C_{60} and phenoxy molecules occur. In the solid phase, crystals of C_{60} and phenol have been successfully obtained, where each C_{60} molecule forms π–π complex units with four phenol molecules, and each of these units is connected with hydrogen bonds between phenol groups to form a distorted square packing of the C_{60} in the crystal's (100) plane with a C_{60}–C_{60} distance of 10.1 Å in one direction and 12.6 Å in the

dx.doi.org/10.1021/la204986n | Langmuir 2012, 28, 4694–4701

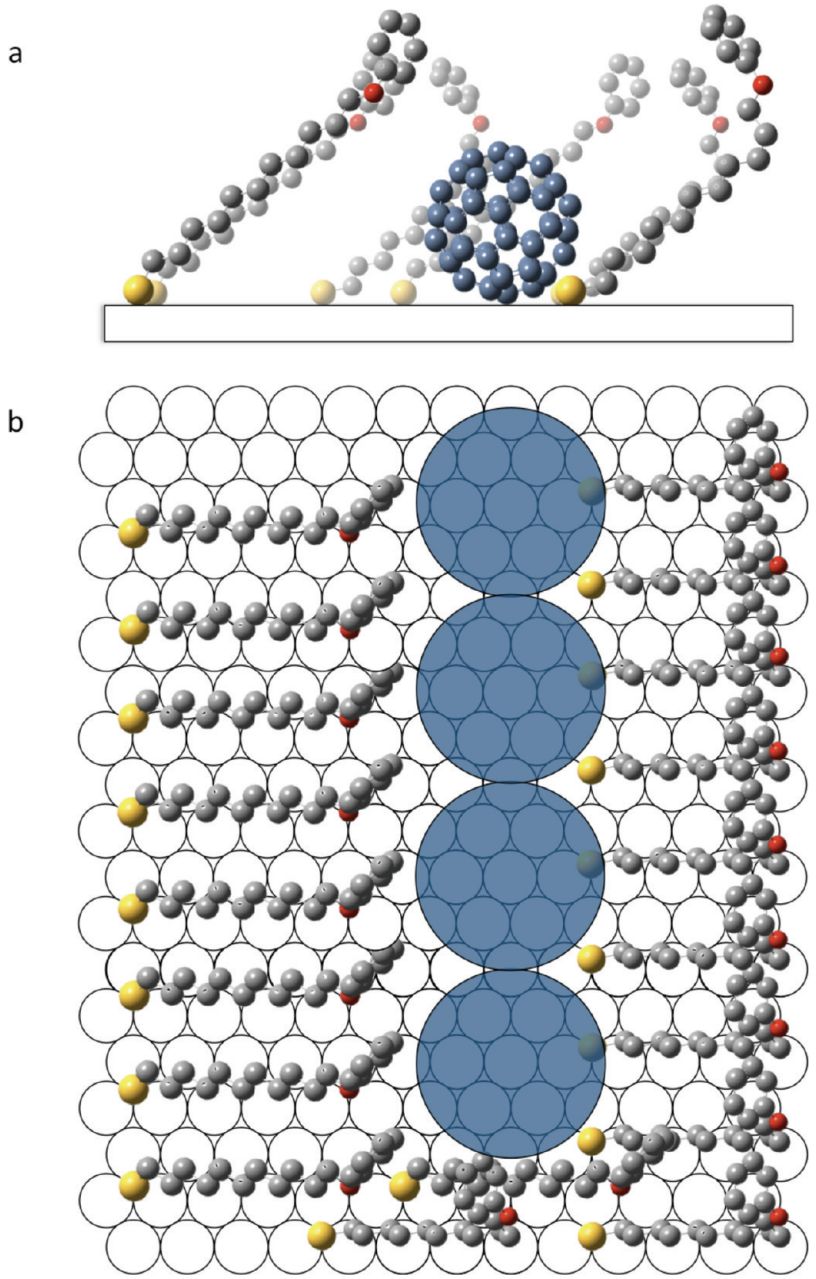

Figure 6. (a) Side view of a schematic of a possible structure of the C_{60} lines, looking directly at the line. The full phenoxy stripes are shown smaller and in a lighter color in the back for clarity of depth. (b) Top view of the same schematic. The transparent dark blue circles represent C_{60} molecules with their van der Waals radius, and the white circles are the Au surface atoms. The C_{60} have been arbitrarily put on an atop site. The full phenoxy stripes are shown at the bottom.

other.[47] In our case, we will not have any hydrogen bonding since we have an ether moiety instead of a hydroxyl group, but it is likely that $\pi-\pi$ interactions between the phenyl rings of the phenoxy group and the C_{60} are responsible for the $(2\sqrt{3} \times 4)$ rectangular packing. Considering a van der Waals diameter of 4.5 Å for an alkyl chain[48] and a typical distance of 3−3.5 Å between a $\pi-\pi$ interacting C_{60} molecule and an arene moiety,[47] the space between the two C_{60} molecules that are 11.5 Å apart is too tight for a phenoxy group to fit in. The phenyl rings could be located anywhere else that satisfies that distance, and the phenoxy molecules are likely to be in a gauche conformation to realize that configuration. The $(2\sqrt{3} \times 4)$ rectangular structure is relatively dense, and there is not enough space for the phenoxy groups to form a cage around individual C_{60} molecules as in the C_{60}-phenol crystal mentioned earlier, especially considering the long alkyl chain of the phenoxy molecule. Within one unit cell, which contains one C_{60} molecule, there is only enough space for one phenoxy molecule, so each C_{60} is only interacting with one phenoxy molecule. This could be the reason why some of the islands started to dissociate easily. C_{60} molecules diffusing by or a C_{60} at the apex of the STM tip could be enough to disturb the island and initiate its disintegration. Our proposed configuration of the phenoxy molecules in the $(2\sqrt{3} \times 4)$ rectangular structure, consistent with all of our data, is shown in Figure 5. The C_{60} and phenyl rings can either be in a face-to-face or edge-to-face configuration, but we have placed them in a face-to-face configuration since it has been noted previously that C_{60}

dx.doi.org/10.1021/la204986n | *Langmuir* 2012, 28, 4694−4701

derivatives containing phenyl rings tend to pack to have face-to-face interactions between the C_{60} and phenyl groups.[49]

Our STS results for the rectangular islands are consistent with this structure as well. There are only two close-packed neighbors for the C_{60} in the $(2\sqrt{3} \times 4)$ rectangular structure, and two more that are slightly farther away, so the LUMO peak shifts higher than for close-packed islands on bare Au(111) due to less shielding effects. The C_{60}–phenoxy π–π interaction most likely causes broadening or perhaps even splitting of the LUMO peak, especially because a molecular state of the phenoxy molecule lies around 0.5 or 1.0 V.[38]

From previous literature, we would expect the C_{60}–phenoxy interaction energy to be on the order of about 1–3 kcal/mol.[49] This is assuming the C_{60}–phenoxy interaction energy is similar to that of C_{60}–pyrrole or C_{60}–thiophene, but slightly smaller due to the phenoxy group's larger size and polarizability.[49−51] The C_{60}–C_{60} dimer interaction energy has been calculated by others to be about 6–10 kcal/mol.[52−54] The C_{60}–C_{60} interaction has a multipole Coulombic component due to the molecules' anisotropic electronic-charge distribution as well as a van der Waals component,[53] while the C_{60}–phenoxy π–π interactions are highly localized compared to the C_{60}–C_{60} interactions. The closer and greater the number of neighboring C_{60} molecules, the greater the total interaction energy for C_{60},[55] so it seems to make more sense energetically for the C_{60} to form hexagonally close-packed islands. However, we did not observe the formation of close-packed islands on initially annealed phenoxy SAMs, which suggests that we also need to consider how the presence of the SAM affects the C_{60} motion during annealing. When the phenoxy SAM that is already in a stable striped phase is annealed again at similar temperatures, the phenoxy molecules are not going to move around as much as they did in the initial anneal. This in turn limits the motion of C_{60} during the anneal, and rearrangement of the molecules probably only occurs around domain boundaries and defect sites. The quenching of fullerene mobility by a low density SAM has also been observed previously for sequential adsorption of octanethiol onto a submonolayer of C_{70}.[46] The phenyl–phenyl interaction within the phenoxy stripes should be about 2.2–2.4 kcal/mol,[56] which is about the same as the C_{60}–phenoxy π–π interactions, so the phenoxy molecules at domain boundaries and defect sites are going to be affected by the presence of C_{60} molecules nearby. However, the chain–chain van der Waals interaction of about 1.4–1.8 kcal/mol per CH_2 will try to keep the phenoxy stripes intact.[57] We believe that a combination of C_{60}–phenoxy interactions and hindered motion due to the phenoxy stripes competes against some of the C_{60}–C_{60} interactions, resulting in the nucleation and growth of unique $(2\sqrt{3} \times 4)$ rectangular islands involving both C_{60}–phenoxy and C_{60}–C_{60} interactions.

When the C_{60} is deposited onto an unannealed phenoxy SAM, they also seem to burrow down to the gold based on the apparent STM heights. Even though the SAM should be denser than the striped phenoxy SAM, it is still not as crystalline as a normal alkanethiol SAM so it should be fairly easy for the C_{60} to find spots to burrow down.[38] Again, the C_{60} are able to move somewhat inside, but their motion is greatly hindered by the SAM.[32,46] When the sample is annealed, a different situation is encountered than if the C_{60} were put on a striped phenoxy SAM. During the anneal, the phenoxy SAM goes through a rather significant transformation from a dense phase similar to that of a normal alkanethiol SAM to a less dense stripe phase involving kinked molecules,[38] so the molecules move around much more. This should allow more movement of the C_{60} as well. Also, as the anneal starts, most of the phenoxy molecules do not have a gauche conformation so the phenoxy groups will be too far from the C_{60} for π–π interactions. Until the phenoxy SAM starts to have a significant amount of kinked molecules, the C_{60} should behave as though they were being annealed in a normal alkanethiol SAM. This explains the formation of many small hexagonally close-packed $(2\sqrt{3} \times 2\sqrt{3})$R30 °$C_{60}$ islands after annealing. The alkyl chains and C_{60} do not interact strongly with each other so they start to phase-separate, which is what others have also observed for C_{60} annealed in an octanethiol SAM.[32,46] In the phenoxy SAM, the $(2\sqrt{3} \times 2\sqrt{3})$R30 °$C_{60}$ islands cannot get too large before their growth is hindered by the formation of the phenoxy stripes around them, which limits the C_{60} motion and introduces phenoxy–C_{60} interactions as mentioned earlier, frequently resulting in triangular islands. The small $(2\sqrt{3} \times 4)$ rectangular islands, found usually at domain boundaries and in etch pits, most likely result from the C_{60} and phenoxy molecules trying to rearrange themselves within a limited space once much of the phenoxy have formed domains of stripes, as in the previous case of C_{60} at defect sites on a striped phenoxy SAM. The single lines of C_{60} were a unique feature, only found when the C_{60} were initially deposited onto an unannealed phenoxy SAM, indicating that the formation of lines involve fairly large concerted motion of both the C_{60} and phenoxy molecules during the formation of the phenoxy stripes. The C_{60} lines seem to hardly disturb the phenoxy stripes around them, so the overall structure of the phenoxy stripes is likely preserved around the lines. One possible conformation is shown in Figure 6. The C_{60} can be adsorbed either on the atop sites of Au(111) as determined by Altman and Colton for the $(2\sqrt{3} \times 2\sqrt{3})$R30° structure[39] or on bridge sites which were calculated to be more energetically favorable by Pérez-Jiménez and co-workers.[45] The C_{60} molecules need to be in a relatively open space because the phenoxy molecules are tilted 50° from the surface normal,[38] not leaving much space for the C_{60} to fit under them.

CONCLUSIONS

C_{60} was solution-deposited onto phenoxy SAMs and studied with UHV-STM and STS. We observed that in the as-deposited state the C_{60} was scattered inside the SAM, but when the samples were annealed in UHV between 350 and 400 K, different C_{60} structures were formed, depending on whether the C_{60} was initially deposited on an unannealed or an annealed phenoxy SAM. On an annealed SAM where the surface consists of a stripe phase, highly unique $(2\sqrt{3} \times 4)$ rectangular islands were observed. We believe that a combination of confined motion at domain boundaries and defect sites and π–π interactions between the phenoxy group and C_{60} are responsible for this structure. On an unannealed SAM, hexagonally close-packed $(2\sqrt{3} \times 2\sqrt{3})$R30° islands and single lines of C_{60} running parallel to the stripes were observed, along with some small $(2\sqrt{3} \times 4)$ rectangular islands. We believe the different structures form as the phenoxy SAM makes a significant structural transformation from a dense phase to a stripe phase during annealing. The C_{60} that were able to segregate from the phenoxy molecules during the initial part of the anneal formed $(2\sqrt{3} \times 2\sqrt{3})$R30° islands, while those that got caught in the middle of the stripe formation inside a domain formed lines. The ones that ended up stuck in domain boundaries or defect sites after most of the stripes had been formed interacted with some of the phenoxy molecules that got

trapped among them and/or with those at the edge of the stripe domains into $(2\sqrt{3} \times 4)$ rectangular islands. Based on the STM apparent heights, STS data, and the fact that all of the C_{60} structures are commensurate with the Au(111) substrate, we concluded that all of the C_{60} are adsorbed directly onto the gold. We believe that by utilizing functionalized SAMs that form stable intermediate phases with mild annealing, the structure and growth of C_{60} can be controlled, which in turn will allow researchers to control the properties of C_{60} on a surface.

AUTHOR INFORMATION

Corresponding Author

*E-mail: s-sibener@uchicago.edu.

Notes

The authors declare no competing financial interest.

ACKNOWLEDGMENTS

This work was funded by the Office of Basic Energy Sciences, Office of Science, U.S. Department of Energy, Grant DE-SC0002583, and infrastructure support from the NSF-Materials Research Science and Engineering Center at The University of Chicago. Seed funding for this work was provided by DTRA, Grant No. HDTRA1-11-1-0001. The authors thank Gaby Avila-Bront for assistance in image processing.

REFERENCES

(1) Kroto, H. W.; Heath, J. R.; O'Brien, S. C.; Curl, R. F.; Smalley, R. E. *Nature* **1985**, *318*, 162.
(2) Arbogast, J. W.; Darmanyan, A. P.; Foote, C. S.; Diederich, F. N.; Whetten, R. L.; Rubin, Y.; Alvarez, M. M.; Anz, S. J. *J. Phys. Chem.* **1991**, *95*, 11.
(3) Ruoff, R. S.; Beach, D.; Cuomo, J.; McGuire, T.; Whetten, R. L.; Diederich, F. *J. Phys. Chem.* **1991**, *95*, 3457.
(4) Wudl, F. *Acc. Chem. Res.* **1992**, *25*, 157.
(5) Fischer, J. E.; Heiney, P. A.; A., B. S. III *Acc. Chem. Res.* **1992**, *25*, 112.
(6) Johansson, M. P.; Jusélius, J.; Sundholm, D. *Angew. Chem., Int. Ed.* **2005**, *44*, 1843.
(7) Talapatra, G. B.; Manickam, N.; Samoc, M.; Orczyk, M. E.; Karna, S. P.; Prasad, P. N. *J. Phys. Chem.* **1992**, *96*, 5206.
(8) Taylor, R.; Walton, D. R. M. *Nature* **1993**, *363*, 685.
(9) Segura, J. L.; Martin, N.; Guldi, D. M. *Chem. Soc. Rev.* **2005**, *34*, 31.
(10) Imahori, H.; Fukuzumi, S. *Adv. Funct. Mater.* **2004**, *14*, 525.
(11) Joachim, C.; Gimzewski, J. K.; Aviram, A. *Nature* **2000**, *408*, 541.
(12) Xie, R.-H.; Bryant, G. W.; Zhao, J.; Vedene H. Smith, J.; Carlo, A. D.; Pecchia, A. *Phys. Rev. Lett.* **2003**, *90*, 206602.
(13) Altman, E. I.; Colton, R. J. *Surf. Sci.* **1993**, *295*, 13.
(14) Gimzewski, J. K.; Modesti, S.; David, T.; Schlittler, R. R. *J. Vac. Sci. Technol. B* **1994**, *12*, 1942.
(15) Abel, M.; Dmitriev, A.; Fasel, R.; Lin, N.; Barth, J. V.; Kern, K. *Phys. Rev. B* **2003**, *67*, 245407.
(16) Hou, J. G.; Yang, J.; Wang, H.; Li, Q.; Zeng, C.; Lin, H.; Bing, W.; Chen, D. M.; Zhu, Q. *Phys. Rev. Lett.* **1999**, *83*, 3001.
(17) Yao, X.; Ruskell, T. G.; Workman, R. K.; Sarid, D.; Chen, D. *Surf. Sci.* **1996**, *366*, L743.
(18) Li, Y. Z.; Patrin, J. C.; Chander, M.; Weaver, J. H.; Chibante, L. P. F.; Smalley, R. E. *Science* **1991**, *252*, 547.
(19) Porath, D.; Levi, Y.; Tarabiah, M.; Millo, O. *Phys. Rev. B* **1997**, *56*, 9829.
(20) Ren, S.; Yang, S.; Zhao, Y. *Langmuir* **2004**, *20*, 3601.
(21) Altman, E. I.; Colton, R. J. *Surf. Sci.* **1992**, *279*, 49.
(22) Schull, G.; Berndt, R. *Phys. Rev. Lett.* **2007**, *99*, 226105.
(23) Zhang, X.; Yin, F.; Palmer, R.; Guo, Q. *Surf. Sci.* **2008**, *602*, 885.
(24) Gardener, J. A.; Briggs, G. A. D.; Castell, M. R. *Phys. Rev. B* **2009**, *80*, 235434.
(25) Torrente, I. F.; Franke, K. J.; Pascual, J. I. *J. Phys.: Condens. Matter* **2008**, *20*, 184001.
(26) Rogero, C.; Pascual, J. I.; Gomez-Herrero, J.; Baro, A. M. *J. Chem. Phys.* **2002**, *116*, 832.
(27) Lu, X.; Grobis, M.; Khoo, K. H.; Louie, S. G.; Crommie, M. *Phys. Rev. B* **2004**, *70*, 115418.
(28) Wang, Y.-B.; Lin, Z. *J. Am. Chem. Soc.* **2003**, *125*, 6072.
(29) Chen, W.; Zhang, H.; Huang, H.; Chen, L.; Wee, A. T. S. *ACS Nano* **2008**, *2*, 693.
(30) Franke, K. J.; Schulze, G.; Henningsen, N.; Fernandez-Torrente, I.; Pascual, J. I.; Zarwell, S.; Rueck-Braun, K.; Cobian, M.; Lorente, N. *Phys. Rev. Lett.* **2008**, *100*, 036807.
(31) Hou, J. G.; Jinlong, Y.; Haiqian, W.; Qunxiang, L.; Changgan, Z.; Lanfeng, Y.; Bing, W.; Chen, D. M.; Qingshi, Z. *Nature* **2001**, *409*, 304.
(32) Li, F.; Tang, L.; Zhou, W.; Guo, Q. *J. Phys. Chem. C* **2009**, *113*, 17899.
(33) Zeng, C.; Wang, H.; Wang, B.; Yang, J.; Hou, J. *Appl. Phys. Lett.* **2000**, *77*, 3595.
(34) Zeng, C.; Wang, B.; Li, B.; Wang, H.; Hou, J. *Appl. Phys. Lett.* **2001**, *79*, 1685.
(35) Caldwell, W. B.; Chen, K.; Mirkin, C. A.; Babinec, S. J. *Langmuir* **1993**, *9*, 1945.
(36) Sahoo, R. R.; Patnaik, A. *J. Colloid Interface Sci.* **2003**, *268*, 43.
(37) Tsukruk, V. V.; Lander, L. M.; Brittain, W. J. *Langmuir* **1994**, *10*, 996.
(38) Nakayama, M.; Kautz, N. A.; Wang, T.; Yuan, H.; Sibener, S. J. *J. Phys. Chem. C* **2012**; DOI: 10.1021/jp212193v.
(39) Altman, E. I.; Colton, R. J. *Phys. Rev. B* **1993**, *48*, 18244.
(40) Cervenka, J.; Flipse, C. F. J. *Nanotechnology* **2010**, *21*, 065302.
(41) Andreev, T.; Barke, I.; Hövel, H. *Phys. Rev. B* **2004**, *70*, 205426.
(42) Hands, I. D.; Dunn, J. L.; Rawlinson, C. S. A.; Bates, C. A. Jahn−Teller Effects in Molecules on Surfaces with Specific Application to C60. In *The Jahn-Teller Effect*; Köppel, H., Yarkony, D. R., Barentzen, H., Eds.; Springer: Berlin, 2009; Vol. *97*, p 517.
(43) Klitsner, T.; Becker, R. S.; Vickers, J. S. *Phys. Rev. B* **1990**, *41*, 3837.
(44) Ege, S. *Organic Chemistry: Structure and Reactivity*, 4th ed.; Houghton Mifflin Co.: Boston, 1999; p 621.
(45) Perez-Jimenez, A. J.; Palacios, J. J.; Louis, E.; SanFabian, E.; Verges, J. A. *ChemPhysChem* **2003**, *4*, 388.
(46) Deering, A.; Kandel, S. *Langmuir* **2006**, *22*, 10025.
(47) Schulz-Dobrick, M.; Panthöfer, M.; Jansen, M. *Eur. J. Inorg. Chem.* **2005**, *2005*, 4064.
(48) Chang, S.; Chao, I.; Tao, Y. *J. Am. Chem. Soc.* **1994**, *116*, 6792.
(49) Fomina, L.; Reyes, A.; Fomine, S. *Int. J. Quantum Chem.* **2002**, *89*, 477.
(50) Abraham, M. H.; McGowan, J. C. *Chromatographia* **1987**, *23*, 243.
(51) Glen, R. C. *J. Comput.-Aided Mol. Des.* **1994**, *8*, 457.
(52) Girifalco, L. A.; Hodak, M.; Lee, R. S. *Phys. Rev. B* **2000**, *62*, 13104.
(53) Hasegawa, M.; Nishidate, K.; Katayama, M.; Inaoka, T. *J. Chem. Phys.* **2003**, *119*, 1386.
(54) Dappe, Y. J.; Ortega, J.; Flores, F. *Phys. Rev. B* **2009**, *79*, 165409.
(55) Guo, S.; Fogarty, D.; Nagel, P.; Kandel, S. *J. Phys. Chem. B* **2004**, *108*, 14074.
(56) Jennings, W. B.; Farrell, B. M.; Malone, J. F. *Acc. Chem. Res.* **2001**, *34*, 885.
(57) Dubois, L. H.; Nuzzo, R. *Annu. Rev. Phys. Chem.* **1992**, *43*, 437.